Cancer Management and Research

Elevate Series

Open Access Full Text Article

ORIGINAL RESEARCH

Parotid Lymph Node Metastasis Prediction of Nasopharyngeal Carcinoma Based on Ultrasound Radiomics Analysis

Xingzhang Long[1,2,*], Yao Xue[1,3,*], Ruhai Zou[1], Shangman Yang[1], Zhong Liu[4], Qicai Huang[4], Chuan Peng[1], Xu Han[1], Weixuan Kong[1], Wei Zheng[1]

[1]Department of Ultrasound, Sun Yat-sen University Cancer Center, State Key Laboratory of Oncology in South China, Collaborative Innovation Center for Cancer Medicine, Guangzhou, People's Republic of China; [2]Department of Ultrasound, Shenzhen Hospital, Southern Medical University, Shenzhen, People's Republic of China; [3]Department of Ultrasound, The Tenth Clinical Medical College of Guangzhou University of Traditional Chinese Medicine, Zhongshan Hospital of Traditional Chinese Medicine, Zhongshan, People's Republic of China; [4]National-Regional Key Technology Engineering Laboratory for Medical Ultrasound, Guangdong Key Laboratory for Biomedical Measurements, and Ultrasound Imaging, School of Biomedical Engineering, Shenzhen University Medical School, Shenzhen University, Shenzhen, People's Republic of China

*These authors contributed equally to this work

Correspondence:Wei Zheng, Department of Ultrasound, Sun Yat-sen University Cancer Center, State Key Laboratory of Oncology in South China, Collaborative Innovation Center for Cancer Medicine, 651 Dongfeng East Road, Guangzhou, 510060, People's Republic of China, Email zhengwei@sysucc.org.cn

Background: To evaluate the clinical utility of ultrasound radiomics in predicting parotid lymph node metastasis (PLNM) in nasopharyngeal carcinoma (NPC) patients.

Methods: Grayscale ultrasound (US) images of parotid gland nodules were segmented, and radiomics features were extracted. An support vector machine (SVM) model was built using the Least Absolute Shrinkage and Selection Operator (LASSO) algorithm for feature selection. Different SVM models were built based on clinical characteristics, radiomics features, and a combination of these features. Performance of the models was assessed using the area under the curve (AUCs), sensitivity and specificity.

Results: Among 406 patients (192 PLNM, 214 benign), a total of 406 nodules were included in this study. Thirty-one radiomics features were selected as significant using the LASSO algorithm from the 474 extracted radiomics features. In the clinical model, NPC patients with suspicious parotid gland nodules of irregular shape, poorly defined margins, long/short axis ratio (LSR) <1, and posterior acoustic enhancement (PAE) were significant variables for PLNM ($p<0.05$). In the validation dataset, the AUC were 0.916 (95% CI: 0.876–0.983) in the clinical model, 0.830 (95% CI: 0.784–0.872) in the single radiomics model, and 0.928 (95% CI: 0.792–0.945) in the combined model. The calibration curve of the different models and decision curve analysis (DCA) demonstrated the diagnostic performance of the combined model.

Conclusion: The combined model using ultrasound radiomics has clinical utility in identifying useful US features and enhancing the diagnostic accuracy of ultrasound for detecting PLNM in patients with NPC.

Keywords: nasopharyngeal carcinoma, parotid lymph node metastasis, ultrasound, radiomics

Introduction

Nasopharyngeal carcinoma (NPC) exhibits a distinct epidemiological pattern, with particularly prevalence in East and Southeast Asia.[1] While cervical lymph node metastasis (CLNM) occurs in approximately 85% of newly diagnosed NPC cases,[2] the parotid lymph nodes are also at risk for metastasis.[3] Importantly, parotid lymph node metastasis (PLNM) is associated with poor prognosis in NPC, necessitating more aggressive therapeutic strategies to reduce distant metastasis.[4,5] However, PLNM occurs in only 1–3.4% of NPC, which is far less than CLNM.[6]

Given NPC's high radiosensitivity, radiotherapy remains the predominant therapeutic modality, with intensity intensity-modulated radiotherapy (IMRT) as the current standard.[2] To minimize radiation-induced toxicities, such as xerostomia, and preserve patients' quality of life, IMRT protocols typically shield the bilateral parotid gland areas. However, overemphasis on safeguarding the parotid gland might lead to post-IMRT PLNM or parotid recurrence.[7]

Received: 18 March 2025
Accepted: 28 August 2025
Published: 13 September 2025

Therefore, it is crucial to detect PLNM prior to radiotherapy. Current radiological diagnosis of PLNM in NPC relies predominantly on computed tomography (CT) or magnetic resonance imaging (MRI) of size and morphological abnormalities.[8] Additionally, metabolic markers from ^{18}F-fluorodeoxyglucose-positron emission tomography/computed tomography (^{18}F-FDG-PET/CT) serve as predictive factors for high-risk recurrence and metastasis.[2] Nevertheless, distinguishing PLNM from primary parotid tumors or benign lymph nodes remains challenging with these modalities.[9]

High-frequency ultrasound (US) offers a practical, high-resolution imaging solution for evaluating parotid nodule (PNs) in superficial soft tissues. While US-guided biopsy is often recommended for suspicious PNs in NPC patients, differentiating metastatic from benign lesions remains difficult due to overlapping imaging features, despite experienced radiologists can identify certain benign nodules based on specific clinical and pathological characteristics.[10] However, reliance on radiologists' experience may lead to bias and subjectivity, highlighting the need for more objective approaches.

Radiomics is an emerging research field that utilizes advanced data characterization algorithms to develop computer-aided diagnosis (CAD) models, enabling the extraction of quantitative imaging biomarkers (radiomic features) from medical images.[11] It enables high-throughput analysis of subtle patterns imperceptible to the human eye.[12] In oncology, tumor heterogeneity is considered as both a prognostic marker and a therapeutic challenge.[13–15] Researches have shown that radiomic features can reflect tumor heterogeneity at the cellular level.[16] More recently, radiomics shows its great diagnostic utility in many diseases including parotid lesions.[17] Based on the reasons upon, radiomics presents great potential for PLNM prediction in NPC. However, existing radiomics research on NPC metastasis focuses on cervical lymph nodes, with few studies addressing PLNM in NPC. Due to its rarity and limited reporting, PLNM is often overlooked, sometimes misclassified as distant metastasis, leading to suboptimal palliative rather than curative management.[9]

To our knowledge, none comprehensive studies have explored the utility of ultrasound-based radiomics analysis for distinguishing PLNM from benign parotid diseases in NPC patients. Hence, this study investigates whether radiomic texture features extracted from high-resolution US images can reliably differentiate PLNM from primary or benign PNs in NPC cases.

Materials and Methods

Study Population

This retrospective study was approved by the Institutional Review Board of our cancer center. The requirement for written informed consent from patients was waived. Patients with a history of NPC who underwent parotid gland nodule ultrasound-guided core needle biopsy between January 2019 and August 2023 were retrospectively evaluated at our institution. Patients with NPC with suspicious PNs revealed by MRI or palpable enlarged PNs underwent ultrasound examination. If suspicious ultrasound signs were detected in PNs, nodule ultrasound-guided biopsy was performed. The inclusion criteria were as follows: (a) age $\geq$ 18 years, (b) history of NPC, and (c) suspected parotid gland nodules that underwent biopsy. The exclusion criteria were as follows: (a) unclear pathological diagnosis; (b) other or unknown pathological types of malignant tumors; and (c) poor image quality. For the positive group, parotid nodules diagnosed as NPC metastasis were enrolled. Conversely, the negative cohort comprised of patients whose nodules were pathologically diagnosed as benign (Figure 1).

Acquisition of Clinical Information and US Image, and General US Features Collection

All patients with suspicious parotid nodules underwent evaluation by an ultrasound doctor with 10 years of experience prior to the ultrasound-guided core needle biopsy. The following devices were used for Conventional US examinations were performed using Aixplorer (Supersonic Imagine), Mylab twice (Esaote), LOGIQ E9 (GE Healthcare), Resona7T (Mindray), and ALOKA (Hitachi Healthcare). A 6–15L linear array probe was used.

The patients lay down on the examination bed in the supine position, and their parotid areas extended well during the US examination. The US features at the largest cross-section of the parotid nodules, including size, shape, boundary, internal echogenicity, posterior acoustic enhancement, and blood flow, were observed and recorded. The largest section of the targeted PN was selected for radiomics analysis from each patient, and the long- and short-axis lengths of the PN were recorded.

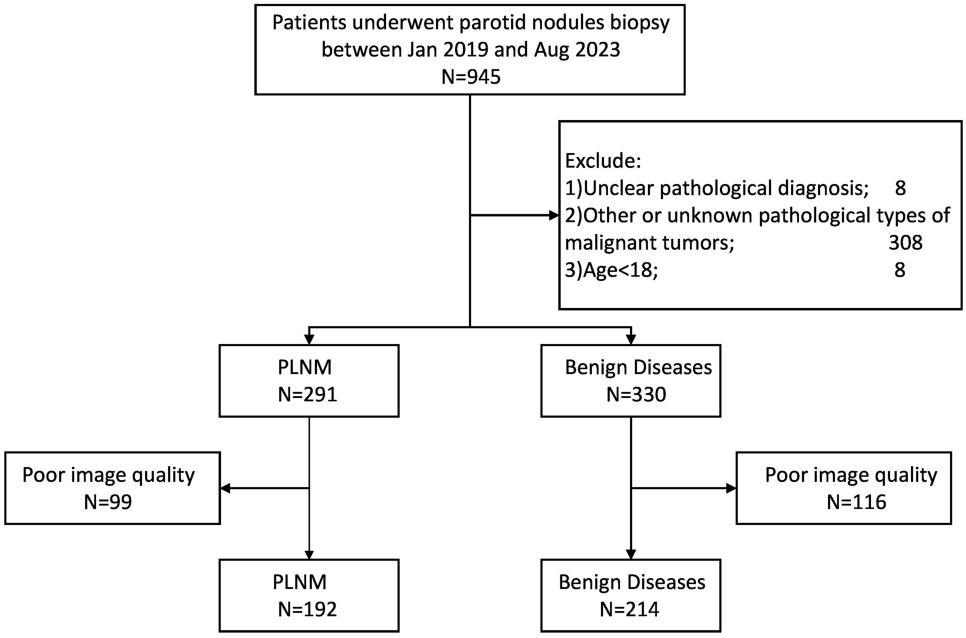

Figure 1 Flowchart of study sample. PLNM= parotid lymph node metastasis. In total, 406 out of 945 patients were included according to the selection criteria.

Demographic and clinical information for all participants was obtained from electronic medical records, and clinical characteristics, such as age, sex (male or female), and smoking status, were recorded. Pathological diagnosis was considered to be the gold standard in our study.

Tumor Segmentation and Feature Extraction

First, the 3D-Slicer software, version 5.4.0 (available at www.slicer.org) was used to segment the regions of interest (ROIs) of 406 lesions. As shown in Figure 2, the ROIs lesions in the largest section were manually outlined by two ultrasound doctors with at least five years of expertise. Second, all the ROIs were verified and corrected by a senior ultrasound physician. Next, radiomics features, including shape, texture, and first-order features, were extracted from the ROIs using the PyRadiomics package in Python, version 3.7.1 (available at https://www.python.org).[17] A cumulative total of 474 radiomic characteristics were extracted from parotid nodules.

Feature Selection and Machine Learning Algorithm Development

The 406 patients involved in this study were randomly sampled and allocated to a training dataset and a test dataset at a proportion of 7:3. First, to reduce the overfitting data dimension and eliminate irrelevant characteristic parameters, a two-independent sample *t*-test was implemented to filter the radiomics features with statistically significant differences ($p < 0.05$). Second, Spearman's rank correlation analysis was applied to eliminate radiomics features with correlations less than 0.9. Third, a penalized logistic regression model employing the Least Absolute Shrinkage and Selection Operator (LASSO), coupled with a five-fold cross-validation procedure, was adopted to select the top-ranked features. Variables related to the PLNM of the NPC were selected by shrinking the coefficient weights to zero. A cross-validation was performed to determine the optimal λ value. The features selected by the LASSO algorithm were then integrated and analyzed using a support vector machine (SVM) classifier. In this study, we built a single radiomics model, and the computed output of this model, known as the radiomics score (Rad-score), was calculated based on the respective coefficient weights of the selected features.

The single radiomics model was an SVM model used for both the training and validation datasets. A clinical model was constructed based on age, sex, smoking history, and several conventional ultrasound characteristics. Characteristics with a p value <0.05, in the univariate logistic regression analysis, were included in the multivariate logistic regression analysis. Variables with a p value <0.05, in the multivariate logistic regression analysis, were deemed to be significant

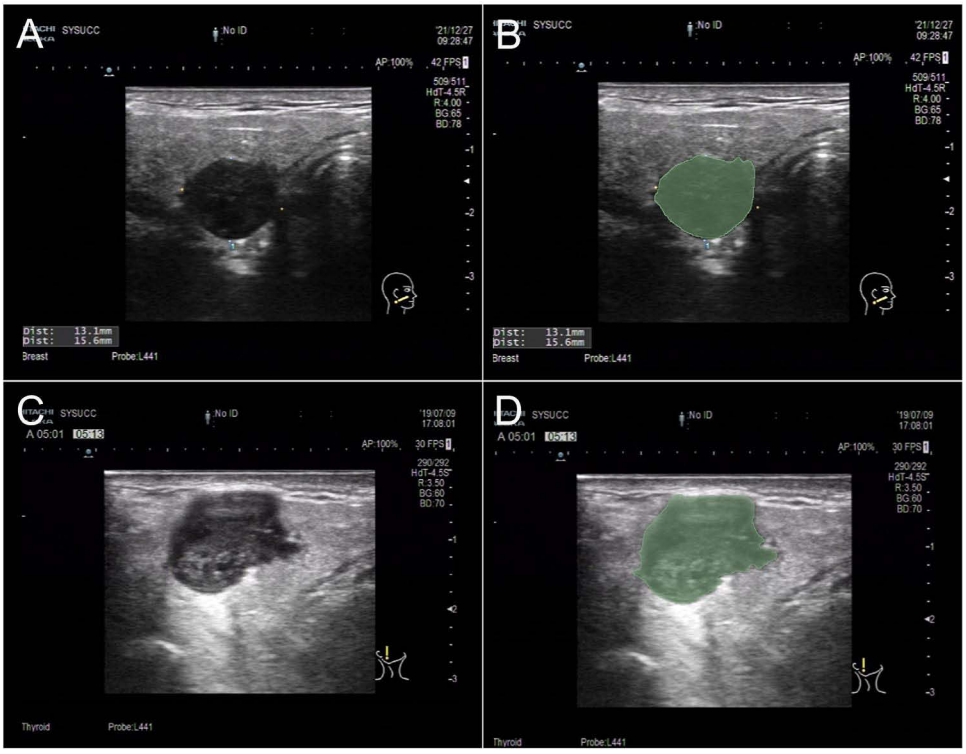

Figure 2 Two examples of delineating region of interest (ROI) on B-mode US images. (**A**) The grayscale US image of a benign parotid nodule enrolled. (**B**) The PLNM was delineated as the ROI. The green region indicated the ROI. (**C** and **D**) the conventional US image and ROI of a metastatic parotid lymph node. The green region in (**D**) indicated the ROI.

predictors for the diagnosis of PLNM of NPC. Combined with the independent factors identified from multivariate logistic regression analysis, we developed a new model based on radiomics model called the combined model. A comparative analysis of the area under the receiver operating characteristic curve (AUC) for the models was performed using Delong's test.

Statistical Analysis

All statistical analyses for this research were conducted using SPSS version 25.0 (IBM) and R version 4.1.2 (available at http://www.r-project.org), and Python version 3.7.1 (available at https://www.python.org). Categorical data are presented as numbers and percentages, whereas continuous variables are presented as mean ± SD/median. The Student's *t*-test was used to assess differences in continuous variables, and the chi-square test or Fisher's test was used to compare categorical variables. Receiver operating characteristic (ROC) curves were used to assess the diagnostic efficacy of the models, with computation of accuracy, sensitivity, specificity, and AUC. Statistical significance was set at $p < 0.05$.

Results

Patient Characteristics

From January 2019 to August 2023, a cumulative total of 945 individuals with suspected PLNM from NPC underwent ultrasound-guided biopsy at our cancer center. Before biopsy, all patients were evaluated by a senior ultrasound doctor to confirm suspicious ultrasound signs of parotid nodules. Poor-quality images and patients with unclear pathological diagnoses or other malignant tumors were excluded. Finally, 192 cases of NPC parotid module metastasis (median age, 49.5 years; interquartile range [IQR], 40.3–58.0 years; 162 men) and 214 cases of benign parotid diseases (median age, 52 years; interquartile range [IQR], 43–60 years; 177 men) were enrolled. Benign parotid diseases include benign parotid lymph nodes, Warthin's tumors, pleomorphic adenomas, and oncocytomas. The clinical characteristics and general ultrasound features of the patients are summarized in Table 1. Significant differences were found between the benign

Table 1 Basic Characteristics and B-Mode Ultrasound Features of 406 Patients

Characteristics	Total	Benign	PLNM	*p*	χ^2
Patient	406	214	192	–	
Gender				0.652	0.204
Male	339 (83.5%)	177 (82.7%)	162 (84.4%)		
Female	67 (16.5%)	37 (17.3%)	30 (15.6%)		
Age*	51 (42, 59)	52 (43, 60)	49.5 (40.25, 58)	0.239	
Unknown	25 (6.2%)	12 (5.6%)	13 (6.8%)		
Long Axis (mm)*	13 (10, 19)	11 (9, 15.25)	16 (12, 25)	<0.001	
Short Axis (mm)*	8 (6, 13)	6 (5, 9)	10 (7, 14)	<0.001	
Long/short Axis Ratio				<0.001	32.470
<1	366 (90.1%)	210 (98.1%)	156 (81.3%)		
>1	40 (9.9%)	4 (1.9%)	36 (18.7%)		
Composition				0.39	1.882
Solid	393 (96.8%)	205 (95.8%)	188 (97.9%)		
Cystic	12 (3.0%)	8 (3.7%)	4 (2.1%)		
Mixed cystic and solid	1 (0.2%)	1 (0.5%)	0		
Internal Echo				<0.001	77.764
Homogeneous	155 (38.2%)	68 (31.8%)	87 (45.3%)		
Hilus clear	87 (21.4%)	82 (38.3%)	5 (1.0%)		
Heterogeneous with unclear hilus	154 (37.9%)	61 (28.5%)	93 (48.4%)		
Heterogeneous with clear hilus	10 (2.5%)	3 (1.4%)	7 (3.6%)		
Shape				<0.001	60.668
Regular	326 (80.3%)	203 (94.9%)	123 (64.1%)		
Irregular	80 (19.7%)	11 (5.1%)	69 (35.9%)		
Margin				<0.001	80.434
Clear	82 (20.2%)	7 (3.3%)	75 (39.1%)		
Blur	324 (79.8%)	207 (96.7%)	117 (60.9%)		
Posterior Acoustic Enhancement				<0.001	61.968
Yes	285 (70.2%)	114 (53.3%)	171 (89.1%)		
No	121 (29.8%)	100 (46.7%)	21 (10.9%)		
Blood Flow				0.001	14.542
None	127 (31.3%)	82 (38.3%)	45 (23.4%)		
Spotted	192 (47.3%)	83 (38.9%)	109 (56.8%)		
Rich	87 (21.4%)	49 (22.9%)	38 (19.8%)		

Note: *Numbers in parentheses are the interquartile ranges.
Abbreviation: PLNM, parotid lymph node metastasis.

and metastatic group, including in the long axis ($p<0.001$), short axis ($p<0.001$), long/short axis ratio ($p<0.001$), internal echo ($p<0.001$), shape ($p<0.001$), and margin ($p<0.001$). Additionally, posterior acoustic enhancement of the parotid lymph nodes was detected in approximately 90% of the metastases. They were larger ($p<0.001$) and had a higher ratio of blur margins ($p<0.001$) and spotted and rich blood flow ($p<0.001$) than the benign group.

Radiomics Feature Selection and Optimal Signature Construction

Demographic characteristics and ultrasound features were evaluated using univariate logistic regression analysis, and variables with $p<0.05$, were subsequently incorporated into the multivariate logistic regression analysis. After multivariate logistic regression, characteristics such as the long/short axis ratio (LSR) ($p = 0.01$), shape ($p = 0.007$), margin ($p<0.001$), and PAE ($p = 0.01$) remained significant factors for PLNM in NPC ($p<0.001$) (Table 2). The AUC values of the clinical model for the training and test cohorts were 0.905 (95% CI: 0.828–0.972) and 0.916 (95% CI: 0.876–0.983), respectively (Table 3).

Table 2 Univariate and Multivariate Logistic Regression of Basic Characteristics and B-Mode Ultrasound Features

Characteristics	Univariate		Multivariate	
	OR (95% CI)	p	OR (95% CI)	p
Gender	1.18 (0.63, 2.22)	0.596		
Age	1.00 (0.98, 1.01)	0.618		
Long Axis (mm)	1.07 (1.04, 1.11)	<0.001	0.97 (0.88, 1.07)	0.522
Short Axis (mm)	1.16 (1.10, 1.23)	<0.001	1.00 (0.85, 1.12)	0.996
LSR	8.65 (2.93, 25.50)	<0.001	6.04 (1.68, 27.79)	0.01
Composition	0.40 (0.10, 1.54)	0.183		
Internal Echo	0.96 (0.74, 1.24)	0.744		
Shape	10.49 (4.55, 24.24)	<0.001	4.66 (1.61, 15.37)	0.007
Margin	0.045 (0.02, 0.13)	<0.001	0.06 (0.01, 0.19)	<0.001
PAE	6.90 (3.69, 12.90)	<0.001	6.54 (2.45, 19.88)	<0.001
Blood Flow	1.24 (0.95, 1.63)	0.117		
Radscore	538.10 (118.62, 2441.00)	<0.001	145.35 (27.75, 921.14)	<0.001

Abbreviations: LSR, Long/short Axis Ratio; PAE, Posterior Acoustic Enhancement.

Table 3 Performance of SVM Models in the Training and Validating Datasets

Model	Training Dataset				Validation Dataset			
	AUC (95% CI)	ACC	Se	Sp	AUC (95% CI)	ACC	Se	Sp
Clinical	0.905 (0.828–0.972)	0.859	0.934	0.833	0.916 (0.876–0.983)	0.776	0.615	0.832
Radiomics	0.811 (0.751–0.854)	0.814	0.672	0.865	0.830 (0.784–0.872)	0.746	0.635	0.785
Combined	0.948 (0.886–0.989)	0.898	0.861	0.911	0.928 (0.792–0.945)	0.836	0.712	0.879

A total of 474 characteristics were obtained from B-mode sonographic images, and the LASSO algorithm was applied to discern 31 radiomic features from this collection. The relevant parameters and coefficients of the LASSO algorithm are shown in Figure 3. An SVM radiomics model was built based on these features, achieving AUC values of 0.811 (95% CI: 0.751–0.854) for the training dataset and 0.830 (95% CI: 0.784–0.872) for the validation dataset (Table 3).

Within the training dataset, the combined model exhibited sensitivity and specificity of 86.1% and 91.1%, respectively. The AUC value of the combined model was 0.948 (95% CI: 88.6–98.9%), which was higher than that of the clinical model (0.948 vs 0.905, $p<0.001$) and the radiomics model (0.948 vs 0.811, $p<0.001$). In the validation dataset, the combined model also obtained the best result, with the highest AUC value compared to that of the radiomics (0.928 vs 0.830, $p<0.001$) and clinical (0.928 vs 0.916, $p<0.001$) models, respectively. Additionally, the combined model demonstrated superior sensitivity compared to the radiomics model (71.2% vs 63.5%), and it also showed better performance in specificity (87.9% vs 78.5%) within the validation cohort.

As shown in Figure 4A and B, the AUC values of the combined model were markedly superior to those of the clinical model in both the training and validation datasets. Additionally, the calibration curve demonstrated the highest accuracy of the combined model for predicting PLNM in NPC patients. As shown in Figure 4C, the calibration curve for the combined model suggested that PLNM prediction in NPC closely approximated the actual outcomes in both the training and validation datasets. The decision curve analysis (DCA) showed the enhanced performance of the combined model within both training and validating cohorts (Figure 4D and E).

The Rad-score for each ultrasound image was determined using the radiomics model. A combined model was then developed by combining clinical predictors with radiomic features. Subsequently, a nomogram was constructed using this combined model. According to the combined model, the LSR, shape, margin, and PAE status of suspicious parotid nodules were independent predictors of PLNM in NPC (Figure 5).

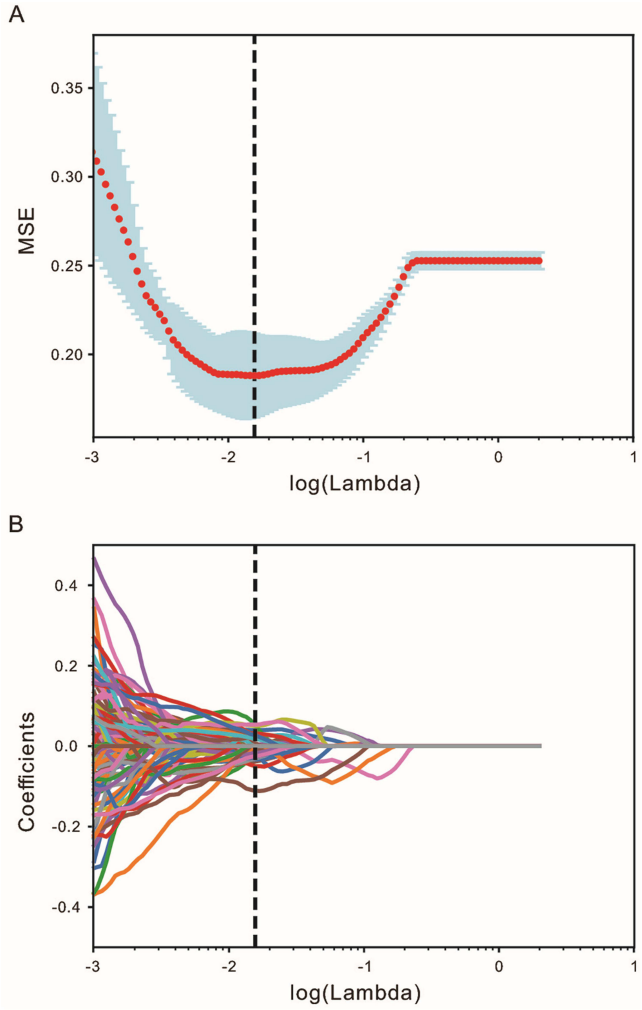

Figure 3 Logistic LASSO regression. (**A**) Cross-validation plot of penalty term. (**B**) LASSO path plot of the model in the training set.

Discussion

To our knowledge, this represents the first study evaluating the utility of ultrasound radiomics for assessing PLNM in NPC, which correlates with increased regional recurrence and disease failure risk.[9] Our findings identified the long/short axis ratio as a crucial predictive factor across all models, with PLNM risk elevated when this ratio < 1. Regarding margin characteristics, irregular or ill-defined margins emerged as significant in both clinical and combined models, contrasting with prior reports of well-defined margins in some lower-grade malignant parotid lesions. In addition, posterior acoustic enhancement proved valuable for differentiating benign nodules from PLNM in NPC patients, which was divergent from previous research.[18] This was potentially attributable to the singular cell type of NPC-related PLNM. Consistent with existing literature, echotexture showed no significant diagnostic value for characterization.[19]

Diverse pathological components of parotid lesions create subtle grayscale ultrasound structural differences Imperceptible to human vision. The diversity of parotid pathologies often yields inconsistent US features even for identical conditions. Therefore, related clinical characteristic analysis is necessary. Radiomics converts images into high-throughput quantitative signatures for deeper biological features analysis. For instance, MRI-based radiomics achieved an AUC of 0.84 for distinguishing PLNM of NPC from benign parotid diseases.[8] Our study focused on the diagnostic potential of ultrasound-based radiomics for NPC-related PLNM, addressing the limitations of conventional visual assessment in detecting subtle pathological features. The development of artificial intelligence now permit quantitative integration of these radiomic

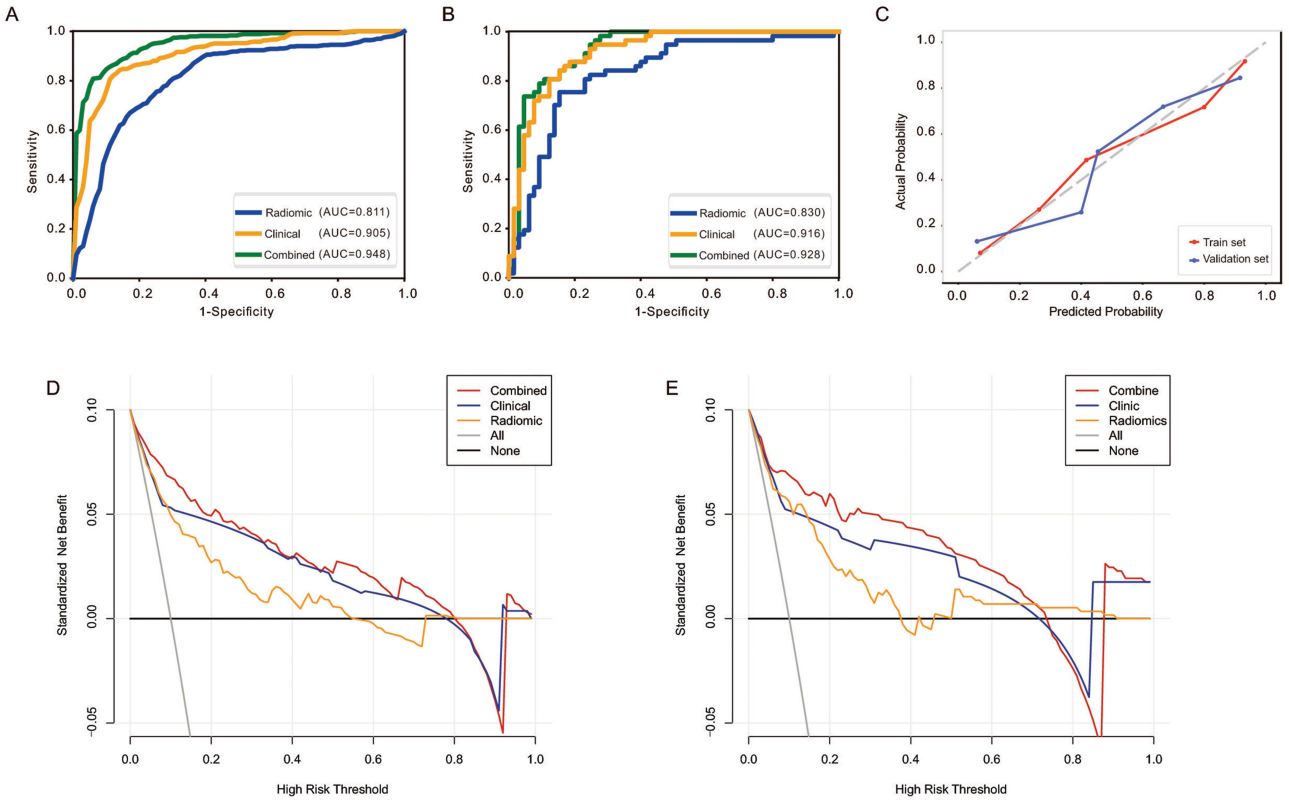

Figure 4 Results of the SVM model. (**A**) The receiver operating characteristics (ROC) of the training dataset. (**B**) The ROC curves of the validation dataset. (**C**) The calibration curve of the combined model. (**D**) The decision curve analysis (DCA) figure of the three models of the training set. (**E**) The DCA figure of the three models of the validation set.

features for PLNM prediction. Prior investigations demonstrated high diagnostic accuracy of conventional US based radiomics in lymph node metastasis.[20,21] Our results suggest ultrasound radiomics could serve as a valuable noninvasive tool for pretreatment assessment of parotid lymph node metastasis in NPC patients. We built and validated radiomics models based on parotid gland nodule features to diagnose PLNM in NPC. The combined prediction model demonstrated outstanding diagnostic performance for PLNM, achieving AUC values of 0.948 in the training cohort and 0.928 in the validation cohort. Notably, the combined model exhibited superior sensitivity (86.1% vs 71.2%) and specificity (91.1% vs 87.9%) in both training and validation cohort compared to other models evaluated in this study.

The heterogeneous pathological composition of parotid lesions results in distinct structural patterns on grayscale ultrasound that often elude conventional visual assessment. This diagnostic challenge is further compounded by: (1) the wide spectrum of parotid pathologies, and (2) the phenotypic variability observed within the same pathological entity. These limitations underscore the critical need for comprehensive clinical-radiological correlation. Our radiomics approach offers particular clinical value by potentially obviating unnecessary core needle biopsies in PLNM-negative cases. Notably, while previous imaging studies of PLNM in NPC have been constrained by small sample sizes (typically <100 cases) and consequent methodological limitations, our investigation employed a substantially larger cohort (n=406), thereby demonstrating the robust predictive performance of ultrasound radiomics for PLNM detection in NPC patients.

However, several limitations of this study should be acknowledged. First, the retrospective design may introduce selection bias and limit generalizability of our findings. Second, as a single-center investigation, external validation through multicenter studies with larger, more diverse patient cohorts is needed to confirm the model's robustness. Third, our radiomics analysis was restricted to conventional grayscale ultrasound features, excluding potentially complementary data from advanced techniques like elastography and contrast-enhanced ultrasound

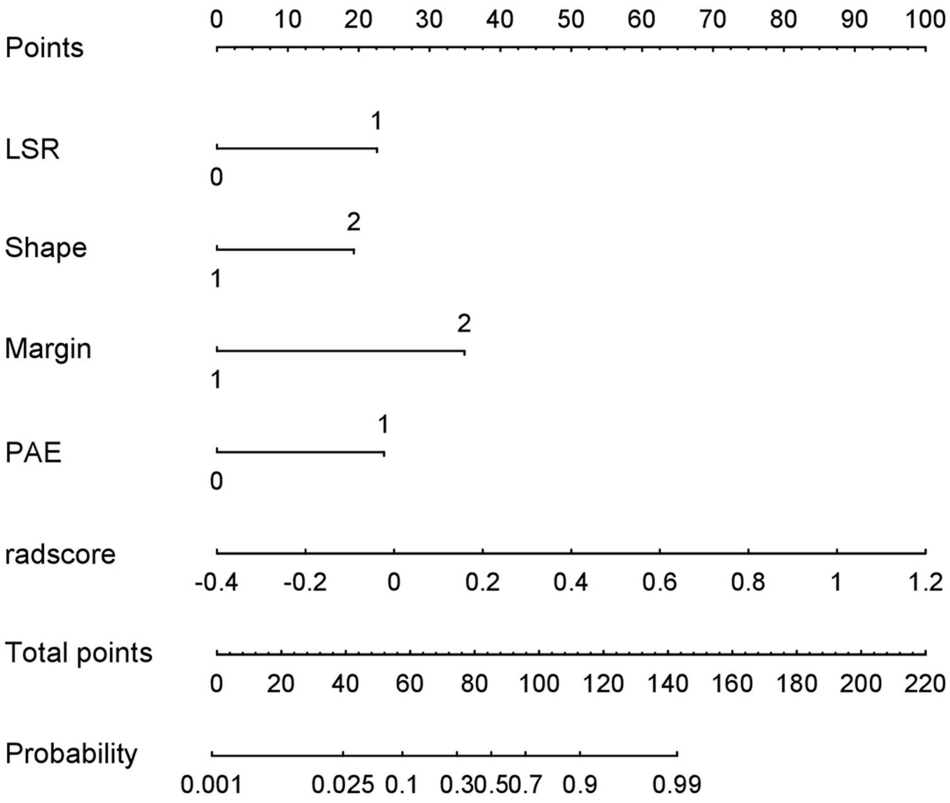

Figure 5 The nomograph based on the combined model.
Abbreviations: LSR, long/short axis ratio; PAE, posterior acoustic enhancement.

(CEUS). While current evidence does not support the diagnostic utility of these modalities for PLNM in NPC, their integration in future radiomics models may provide incremental value.

Conclusion

In summary, our SVM-based radiomics model demonstrates that combining ultrasound features such as irregular shape, blur margin, long/short axis ratio <1, and posterior acoustic enhancement significantly improves PLNM detection in NPC.

Data Sharing Statement

Data supporting the findings of this study are available from the corresponding author upon reasonable request.

Ethics Approval and Consent to Participate

This study was approved by the Institutional Review Board (IRB) of the Sun Yat-sen University Cancer Center (approval reference 20240110102000047857O). The requirement for informed consent was formally waived by our Institutional Review Board (IRB) because: a) the research involved no more than minimal risk to subjects, b) the waiver did not adversely affect subjects' rights and welfare, c) the research could not practicably be carried out without the waiver. All patient data were anonymized and handled with strict confidentiality throughout the study. This study was conducted in accordance with the Declaration of Helsinki.

Author Contributions

All authors made a significant contribution to the work reported, whether that is in the conception, study design, execution, acquisition of data, analysis and interpretation, or in all these areas; took part in drafting, revising or critically reviewing the article; gave final approval of the version to be published; have agreed on the journal to which the article has been submitted; and agree to be accountable for all aspects of the work.

Funding

This study was supported by the National Natural Science Foundation of China (No. 82171957) and National Natural Science Foundation of China (No. 82202179).

Disclosure

The authors declare no conflicts of interest in this work.

References

1. Bossi P, Chan AT, Licitra L, et al. Nasopharyngeal carcinoma: ESMO-EURACAN Clinical Practice Guidelines for diagnosis, treatment and follow-up(dagger). *Ann Oncol*. 2021;32(4):452–465. doi:10.1016/j.annonc.2020.12.007
2. Chen YP, Chan A, Le QT, Blanchard P, Sun Y, Ma J. Nasopharyngeal carcinoma. *Lancet*. 2019;394(10192):64–80. doi:10.1016/S0140-6736(19)30956-0
3. Lin C, Lu N, Liang JL, et al. Clinical treatment considerations in the intensity-modulated radiotherapy era for parotid lymph node metastasis in patients with nasopharyngeal carcinoma. *Radiother Oncol*. 2023;186:109802. doi:10.1016/j.radonc.2023.109802
4. Xu Y, Chen X, Zhang M, et al. Prognostic effect of parotid area lymph node metastases after preliminary diagnosis of nasopharyngeal carcinoma: a propensity score matching study. *Cancer Med*. 2017;6(10):2213–2221. doi:10.1002/cam4.1154
5. Lin C, Sun XS, Liu SL, et al. Establishment and validation of a nomogram for nasopharyngeal carcinoma patients concerning the prognostic effect of parotid lymph node metastases. *Cancer Res Treat*. 2020;52(3):855–866. doi:10.4143/crt.2019.772
6. Wang HZ, Cao CN, Luo JW, et al. High-risk factors of parotid lymph node metastasis in nasopharyngeal carcinoma: a case-control study. *Radiat Oncol*. 2016;11(1):113. doi:10.1186/s13014-016-0691-x
7. Cao CN, Luo JW, Gao L, et al. Clinical characteristics and patterns of failure in the parotid region after intensity-modulated radiotherapy for nasopharyngeal carcinoma. *Oral Oncol*. 2013;49(6):611–614. doi:10.1016/j.oraloncology.2013.02.001
8. Chen C, Lin Z, Xiao Y, et al. Role of diffusion-weighted imaging in the discrimination of benign and metastatic parotid area lymph nodes in patients with nasopharyngeal carcinoma. *Sci Rep*. 2018;8(1):281. doi:10.1038/s41598-017-18617-y
9. Zhang Y, Zhang ZC, Li WF, Liu X, Liu Q, Ma J. Prognosis and staging of parotid lymph node metastasis in nasopharyngeal carcinoma: an analysis in 10,126 patients. *Oral Oncol*. 2019;95:150–156. doi:10.1016/j.oraloncology.2019.06.013
10. Rzepakowska A, Osuch-Wojcikiewicz E, Sobol M, Cruz R, Sielska-Badurek E, Niemczyk K. The differential diagnosis of parotid gland tumors with high-resolution ultrasound in otolaryngological practice. *Eur Arch Otorhinolaryngol*. 2017;274(8):3231–3240. doi:10.1007/s00405-017-4636-2
11. Mayerhoefer ME, Materka A, Langs G, et al. Introduction to radiomics. *J Nucl Med*. 2020;61(4):488–495. doi:10.2967/jnumed.118.222893
12. Gillies RJ, Kinahan PE, Hricak H. Radiomics: images are more than pictures, they are data. *Radiology*. 2016;278(2):563–577. doi:10.1148/radiol.2015151169
13. Burrell RA, McGranahan N, Bartek J, Swanton C. The causes and consequences of genetic heterogeneity in cancer evolution. *Nature*. 2013;501(7467):338–345. doi:10.1038/nature12625
14. Yang F, Wang Y, Li Q, et al. Intratumor heterogeneity predicts metastasis of triple-negative breast cancer. *Carcinogenesis*. 2017;38(9):900–909. doi:10.1093/carcin/bgx071
15. Liu J, Dang H, Wang XW. The significance of intertumor and intratumor heterogeneity in liver cancer. *Exp Mol Med*. 2018;50(1):e416. doi:10.1038/emm.2017.165
16. Moon SH, Kim J, Joung JG, et al. Correlations between metabolic texture features, genetic heterogeneity, and mutation burden in patients with lung cancer. *Eur J Nucl Med Mol Imaging*. 2019;46(2):446–454. doi:10.1007/s00259-018-4138-5
17. Li Q, Jiang T, Zhang C, et al. A nomogram based on clinical information, conventional ultrasound and radiomics improves prediction of malignant parotid gland lesions. *Cancer Lett*. 2022;527:107–114. doi:10.1016/j.canlet.2021.12.015
18. Kovacevic DO, Fabijanic I. Sonographic diagnosis of parotid gland lesions: correlation with the results of sonographically guided fine-needle aspiration biopsy. *J Clin Ultrasound*. 2010;38(6):294–298. doi:10.1002/jcu.20704
19. Lamont JP, McCarty TM, Fisher TL, Kuhn JA. Prospective evaluation of office-based parotid ultrasound. *Ann Surg Oncol*. 2001;8(9):720–722. doi:10.1007/s10434-001-0720-2
20. Yu J, Deng Y, Liu T, et al. Lymph node metastasis prediction of papillary thyroid carcinoma based on transfer learning radiomics. *Nat Commun*. 2020;11(1):4807. doi:10.1038/s41467-020-18497-3
21. Zheng X, Yao Z, Huang Y, et al. Deep learning radiomics can predict axillary lymph node status in early-stage breast cancer. *Nat Commun*. 2020;11(1):1236. doi:10.1038/s41467-020-15027-z